Tracing photon transmission in dye-doped DNA-CTMA optical nanofibers

Weihong Long, Weiwen Zou,[*] Xing Li, Wenning Jiang, Xinwan Li, and Jianping Chen

State Key Laboratory of Advanced Optical Communication Systems and Networks, Department of Electronic Engineering, Shanghai Jiao Tong University, Shanghai 200240, China
[*]*wzou@sjtu.edu.cn*

Abstract: We experimentally demonstrate the novel phenomena of photoluminescence (PL) and fluorescence resonance energy transfer (FRET) assisted three-color PL separating in DNA optical nanofibers consisting of the stretched and connected DNA-cetyltrimethyl ammonium wires. The PL experiments are performed to comparatively trace photon transmission between single dye-doped DNA-CTMA optical nanofiber and PMMA optical nanofiber. A cascade FRET including DNA minor groove binder and DNA intercalators is used to further trace photon transmission inside DNA-CTMA wire. These experimental results will help to intrigue the new applications of DNA-CTMA as molecular waveguide in optobioelectronics area.

©2014 Optical Society of America

OCIS codes: (230.7370) Waveguides; (170.5280) Photon migration; (250.5230) Photoluminescence.

References and links

1. J. Bath and A. J. Turberfield, "DNA nanomachines," Nat. Nanotechnol. **2**(5), 275–284 (2007).
2. A. V. Pinheiro, D. Han, W. M. Shih, and H. Yan, "Challenges and opportunities for structural DNA nanotechnology," Nat. Nanotechnol. **6**(12), 763–772 (2011).
3. W. Su, V. Bonnard, and G. A. Burley, "DNA-templated photonic arrays and assemblies: design principles and future opportunities," Chemistry **17**(29), 7982–7991 (2011).
4. M. Heilemann, P. Tinnefeld, G. Sanchez Mosteiro, M. Garcia Parajo, N. F. Van Hulst, and M. Sauer, "Multistep energy transfer in single molecular photonic wires," J. Am. Chem. Soc. **126**(21), 6514–6515 (2004).
5. J. K. Hannestad, P. Sandin, and B. Albinsson, "Self-assembled DNA photonic wire for long-range energy transfer," J. Am. Chem. Soc. **130**(47), 15889–15895 (2008).
6. K. Boeneman, D. E. Prasuhn, J. B. Blanco-Canosa, P. E. Dawson, J. S. Melinger, M. Ancona, M. H. Stewart, K. Susumu, A. Huston, and I. L. Medintz, "Self-assembled quantum dot-sensitized multivalent DNA photonic wires," J. Am. Chem. Soc. **132**(51), 18177–18190 (2010).
7. W. Su, M. Schuster, C. R. Bagshaw, U. Rant, and G. A. Burley, "Site-specific assembly of DNA-based photonic wires by using programmable polyamides," Angew. Chem. Int. Ed. Engl. **50**(12), 2712–2715 (2011).
8. W. Su, C. R. Bagshaw, and G. A. Burley, "Addressable and unidirectional energy transfer along a DNA three-way junction programmed by pyrrole-imidazole polyamides," Sci Rep **3**, 1883 (2013).
9. A. J. Steckl, "DNA - a new material for photonics?" Nat. Photonics **1**(1), 3–5 (2007).
10. D. Madhwal, I. Singh, J. Kumar, C. S. Bhatia, P. K. Bhatnagar, and P. C. Mathur, "Increasing the luminous efficiency of an MEH-PPV based PLED using salmon DNA and single walled carbon nanotube," J. Lumin. **131**(7), 1264–1266 (2011).
11. H. You, H. Spaeth, V. N. Linhard, and A. J. Steckl, "Role of surfactants in the interaction of dye molecules in natural DNA polymers," Langmuir **25**(19), 11698–11702 (2009).
12. L. Tong, R. R. Gattass, J. B. Ashcom, S. He, J. Lou, M. Shen, I. Maxwell, and E. Mazur, "Subwavelength-diameter silica wires for low-loss optical wave guiding," Nature **426**(6968), 816–819 (2003).
13. G. Brambilla, "Optical fibre nanowires and microwires: a review," J. Opt. **12**(4), 043001 (2010).
14. W. Long, W. Zou, X. Li, and J. Chen, "DNA optical nanofibers: preparation and characterization," Opt. Express **20**(16), 18188–18193 (2012).
15. J. Hu, Y. Zhang, H. Gao, M. Li, and U. Hartmann, "Artificial DNA patterns by mechanical nanomanipulation," Nano Lett. **2**(1), 55–57 (2002).
16. A. Rajendran, M. Endo, and H. Sugiyama, "Single-molecule analysis using DNA origami," Angew. Chem. Int. Ed. Engl. **51**(4), 874–890 (2012).
17. S. Kumar and G. Mishra, "Stretching single stranded DNA," Soft Matter **7**(10), 4595–4605 (2011).

18. C. J. Murphy, M. R. Arkin, Y. Jenkins, N. D. Ghatlia, S. H. Bossmann, N. J. Turro, and J. K. Barton, "Long-range photoinduced electron transfer through a DNA helix," Science **262**(5136), 1025–1029 (1993).
19. J. A. Berashevich and T. Chakraborty, "Influence of solvent on the energetics of hole transfer in DNA," J. Phys. Chem. B **111**(47), 13465–13471 (2007).
20. C. Yang, D. Moses, and A. J. Heeger, "Base-pair stacking in oriented films of DNA–surfactant complex," Adv. Mater. **15**(16), 1364–1367 (2003).
21. J. K. Hannestad, S. R. Gerrard, T. Brown, and B. Albinsson, "Self-assembled DNA-based fluorescence waveguide with selectable output," Small **7**(22), 3178–3185 (2011).
22. A. S. Finch, C. M. Anton, C. M. Jacob, T. J. Proctor, and D. N. Stratis-Cullum, "Assembly of DNA architectures in a non-aqueous solution," Nanomaterials **2**(4), 275–285 (2012).
23. S. O. Kelley and J. K. Barton, "Electron transfer between bases in double helical DNA," Science **283**(5400), 375–381 (1999).
24. T. Lin, I. Chen, and Y. Hung, "Hole mobility characterization of DNA biopolymer by time-of-flight technique," Appl. Phys. Lett. **101**(15), 153701 (2012).
25. S. Uphoff, S. J. Holden, L. Le Reste, J. Periz, S. van de Linde, M. Heilemann, and A. N. Kapanidis, "Monitoring multiple distances within a single molecule using switchable FRET," Nat. Methods **7**(10), 831–836 (2010).
26. S. S. Vogel, C. Thaler, and S. V. Koushik, "Fanciful FRET," Sci. STKE **331**(re2), 1–8 (2006).
27. Y. Ner, J. G. Grote, J. A. Stuart, and G. A. Sotzing, "White luminescence from multiple-dye-doped electrospun DNA nanofibers by fluorescence resonance energy transfer," Angew. Chem. Int. Ed. Engl. **48**(28), 5134–5138 (2009).
28. D. Navarathne, Y. Ner, J. G. Grote, and G. A. Sotzing, "Three dye energy transfer cascade within DNA thin films," Chem. Commun. (Camb.) **47**(44), 12125–12127 (2011).
29. K. S. Sanju, P. P. Neelakandan, and D. Ramaiah, "DNA-assisted white light emission through FRET," Chem. Commun. (Camb.) **47**(4), 1288–1290 (2011).
30. M. Ibisate, J. F. Galisteo-López, V. Esteso, and C. López, "FRET-mediated amplified spontaneous emission in DNA–CTMA complexes," Adv. Opt. Mater. **1**(9), 651–656 (2013).
31. P. D. Sahare, V. K. Sharma, D. Mohan, and A. A. Rupasov, "Energy transfer studies in binary dye solution mixtures: acriflavine+rhodamine 6G and acriflavine+rhodamine B," Spectrochim. Acta A Mol. Biomol. Spectrosc. **69**(4), 1257–1264 (2008).
32. N. Kitazawa, W. Aroonjaeng, M. Aono, and Y. Watanabe, "Synthesis and luminescence properties of dye-doped deoxyribonucleic acid films," J. Lumin. **132**(6), 1432–1436 (2012).
33. F. M. Ho and E. A. H. Hall, "A strand exchange FRET assay for DNA," Biosens. Bioelectron. **20**(5), 1001–1010 (2004).
34. G. S. Khan, A. Shah, Zia-ur-Rehman, and D. Barker, "Chemistry of DNA minor groove binding agents," J. Photochem. Photobiol. B **115**, 105–118 (2012).
35. Y. Kawabe, L. Wang, S. Horinouchi, and N. Ogata, "Amplified spontaneous emission from fluorescent-dye-doped DNA–surfactant complex films," Adv. Mater. **12**(17), 1281–1283 (2000).
36. Y. Guan, R. Shi, X. Li, M. Zhao, and Y. Li, "Multiple binding modes for dicationic hoechst 33258 to DNA," J. Phys. Chem. B **111**(25), 7336–7344 (2007).
37. G. Duportail, Y. Mauss, and J. Chambron, "Quantum yields and fluorescence lifetimes of acridine derivatives interacting with DNA," Biopolymers **16**(7), 1397–1413 (1977).
38. K. A. Selanger, J. Falnes, and T. Sikkeland, "Fluorescence lifetime studies of rhodamine 6G in methanol," J. Phys. Chem. **81**(20), 1960–1963 (1977).
39. Y. D. Lantukh, S. N. Pashkevich, S. N. Letuta, E. K. Alidzhanov, and A. A. Kul'sarin, "Spectroscopic properties of DNA-acridine orange biopolymer films," Opt. Spectrosc. **110**(6), 880–884 (2011).
40. Y. Kwon, D. Choi, J. I. Jin, C. Lee, E. Koh, and J. Grote, "Comparison of magnetic properties of DNA-cetyltrimethyl ammonium complex with those of natural DNA," Sci. China Chem. **55**(5), 814–821 (2012).
41. F. D. Lewis, T. Wu, Y. Zhang, R. L. Letsinger, S. R. Greenfield, and M. R. Wasielewski, "Distance-dependent electron transfer in DNA hairpins," Science **277**(5326), 673–676 (1997).

1. Introduction

DNA, as the building blocks of molecular devices [1–3], has significant applications in biophotonics and nanophotonics [4–8]. For example, DNA-cetyltrimethyl ammonium (CTMA), can enhance light emission greatly and is emerging as a promising candidate for bio-organic light-emitting diodes (BioLEDs) and polymer light-emitting diodes (PLEDs) [9,10]. However, inherent mechanism of its optoelectronic properties has not been explored thoroughly [9,11]. The related researches indicate the novel material properties may results from photon transmission related to the structure of DNA-CTMA wire [11]. It has been shown that nanoscale optical fibers offer feasibility to trace photon transmission because of its distinctive features such as low loss, configurability and high flexibility [12,13]. Based on the above mentioned reasons and our previous work [14], we experimentally demonstrate and theoretically interpret the novel phenomena in DNA-CTMA nanofiber consisting of the

stretched and connected DNA molecular wire. We clearly trace photon transmission in DNA-CTMA via DNA minor groove binder, DNA intercalator and three-dye cascade fluorescence resonance energy transfer (FRET). We prove that such DNA-CTMA is of molecular waveguide with low loss, which will open the door to develop new optoelectronic devices and applications based on DNA nanostructures, such as molecular optical switches and the potential solution to promote external quantum efficiency of organic light-emitting diodes (OLEDs).

In order to trace the photon transmission in DNA-CTMA, it is crucial to prepare the high quality DNA wire and have an efficient method to trace the photons. Effective tracing requires that DNA molecule be stretched or dispersed [15–17]. Up to date, the most common method is to disperse DNA in aqueous solution where photon transmission can be confirmed indirectly by monitoring the spectra of the tracers [5,18]. However, these DNA molecules are disordered because of Brownian motion, which makes the direct observation impossible. Furthermore, there are two problems. Firstly, as a polar molecule, H_2O suppresses charge dislocation and photoinduced charge transmission in DNA [19]. Secondly, the short length of a single DNA molecule, which is normally hundreds of nanometers, makes it difficult to carry out the direct observation under normal conditions. The related work hints that the two problems may be solved by aligning DNA helices along the axis of the double helix and nanoassembling in non-aqueous solution [14,20], which differentiates from the nanoassembly in aqueous solution [8,21]. The transformation of DNA nanomaterials from aqueous solution to non-aqueous solution has been principally demonstrated recently [22]. Such transformation provides a new way to put the existing DNA intelligent nanostructures into optoelectronic applications. Our previous experiments of light transmission and the other studies indirectly hint that photons transmit inside DNA-CTMA [14,23,24]. Thereby, there is an urgency to experimentally probe the inherent optical mechanism of DNA-CTMA wire.

In this paper, we prove that the DNA-CTMA molecular wire is of waveguide structure, which can be stretched via connecting and assembling into a nanofiber. We explore photon transmission inside the stretched DNA-CTMA molecular waveguide by employing single dye and three dye cascade FRET, a valid tool to probe molecular structures either with respect to distance information and dynamic behavior of the targeted molecule [25,26]. Recently, two or three-step FRET has been performed in different DNA-CTMA matrices [27–30]. However, it cannot reflect the molecular spatial difference because the FRET-mediated photoluminescence (PL) is just the accumulation of independent FRETs in the disordered DNA-CTMA wires. In contrast, DNA-CTMA wires we prepared are paralleled and partially connected in the optical nanofiber when viscous DNA-CTMA solution was physically drawn with a tungsten probe. Assembling DNA-CTMA molecules into a nanofiber eliminates the length limitation of a single DNA-CTMA molecule and the prolonged FRET amplifies the position difference of DNA binders by extending the distance of photon transmission.

2. Tracing photon transmission in single dye doped DNA optical nanofibers

A DNA molecular waveguide we prepared is illustrated in Fig. 1(a). It consists of a DNA double strand wrapped by CTMA groups. The DNA-CTMA molecules are stretched via directly drawing DNA-CTMA solution. We used tiny proportion of decamethonium to enhance the viscosity of DNA-CTMA molecules. DNA solution was mixed with the lipid solution with cetyltrimethyl ammonium and decamethonium molar ratio: 20: 1. They are rather stable. The pure DNA sample was used for about one year and the doping sample for two months. Other preparation procedures of DNA-CTMA optical fiber were the same as our previous work [14]. In the course of drawing, they self-assembled into a DNA-CTMA nanofiber. The lengths range from several micrometers to several centimeters. Figure 1(b) is the schematic view of the self-assembled DNA-CTMA nanofiber with a diameter of about 600 nm. CTMA groups surround DNA (Fig. 1(a)) and neutralize phosphate backbone, which improves the surface smoothness of DNA-CTMA nanofibers as shown by the field-emission

scanning electron microscopy (NOVA NanoSEM 230) and transmission electron microscopy (JEOL JEM-2010HT) images (Figs. 1(c)-1(d)). We used two typical kinds of photon tracers, i.e. Rhodamine 6G (R6G) (DNA intercalator) and Hoechst 33258 (minor groove binder), to monitor photon transmission [31–34]. We also designed a cascade FRET to further probe inherent mechanism of DNA-CTMA material. Owing to the longitudinal nature of the assembled DNA-CTMA nanofiber, we are able to find the essential differences via the interaction between photons and the dyes, including a novel phenomenon of FRET-assisted PL separation originating from the position difference of dyes in DNA molecular waveguide.

We employ R6G for its high quantum yield as one tracer to compare the different optical behaviors in DNA-CTMA and polymethylmethacrylate (PMMA) [31]. The excitation laser from light sources was launched into the fiber taper coupled with DNA-CTMA fiber through an objective. The PL signals were collected by an objective (Olympus, NA = 0.9) and directed through a dichroic mirror and the notch filter consistent with the excitation laser. The filtered light was then split by a beam splitter and directed to a spectrometer and a CCD camera for spectral and image measurement, respectively. All of the optical measurements of the DNA-CTMA nanofibers were performed under the optical microscope at room temperature and with normal pressure. All of the laser excitation tests were carried out in dark room. The experimental results show that the PL in R6G-DNA-CTMA moved much more rapid even with less excitation power than that in R6G doped PMMA nanofiber (see Figs. 2(a)-2(d)), indicating that the interaction between photons and R6G molecules in DNA-CTMA nanofiber is more effective than that in PMMA. The PL moving is actually the spatial evolution of the successive excitation and bleaching of R6G. Referred to the fact that R6G molecules can intercalate into DNA (see the schematic view, Fig. 3(a)) while they distribute uniformly in PMMA [35], it is reasonable to speculate that photon transmission occurred along DNA-CTMA molecular wire. We qualitatively observed the dependence of PL moving speed on the doping concentration and found that it decreased when the concentration of R6G increased in both nanofibers.

Hoechst 33258 was used as another tracer to study the photon transmission (see Fig. 3(b) for schematic illustration). The position difference of Hoechst 33258 and R6G anchored to DNA-CTMA molecular wire is schematically compared in Fig. 3(c). Hoechst 33258-DNA-CTMA molecular wire likes an optical fiber (waveguide) with doped cladding while R6G-DNA-CTMA molecular wire likes an optical fiber with doped core. Figures 4(a)-4(e) are the PL microscope images, PL moving distance vs. time and the PL spectrum of R6G-DNA-CTMA complexes and Hoechst 33258-DNA-CTMA complexes, respectively. Figure 4(d) shows the PL image of Hoechst 33258-DNA-CTMA nanofiber in the bright background (up) and the PL image in the dark background (down). In comparison, there are two significant differences. The first is the shape of the PL microscope images. It is a bright point for R6G-DNA-CTMA nanofiber (see Fig. 4(a)), while a short line for Hoechst 33258-DNA-CTMA nanofiber (see Fig. 4(d)). The second is the moving speed. The PL moving speed of Hoechst 33258-DNA-CTMA nanofiber was very slow compared with that of R6G-DNA-CTMA nanofiber. It took several hours to transmit the same distance as in R6G-DNA-CTMA nanofiber. Such differences arise from the different anchoring positions of the photon tracers. R6G anchored to the core and thus blocked the photon propagating along the core until being bleached. Therefore the PL microscope image is a bright point. In contrast, Hoechst 33258 anchoring to the cladding was excited and bleached by less excitation energy density of the optical evanescence field. Such interaction took place in a relatively long distance, which explains why the PL is a short line as depicted in Fig. 4(d). This also explains the PL moving speed of R6G-DNA-CTMA nanofiber is quicker than that of Hoechst 33258-DNA-CTMA nanofiber since the former was excited under stronger power density. Such difference is also reflected by the spectra. The peak value of PL intensity of R6G-DNA-CTMA nanofiber is higher and increases with high excitation power density (see Fig. 4(c)), while that of Hoechst

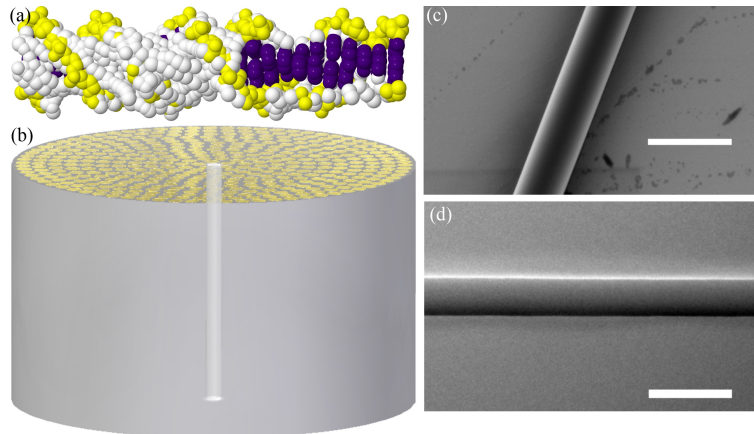33258-DNA-CTMA nanofiber is relatively weak even excited by high power density (see Fig. 4(e)).

Fig. 1. Images of DNA-CTMA molecular waveguide and DNA-CTMA nanofibers. (a) Schematic image of a DNA molecular waveguide, right part is the cutaway view. CTMA groups: white; phosphate backbone: yellow; DNA base pairs: indigo. (b) Sectional schematic view of DNA-CTMA nanofiber, the surfaced tube is a DNA-CTMA molecular waveguide. (c) SEM image of a 560-nm-diameter DNA-CTMA nanofiber on the surface of silicon wafer. (d) TEM image of a 400-nm-diameter dye-doped DNA-CTMA nanofiber. Scale bar: 1 μm.
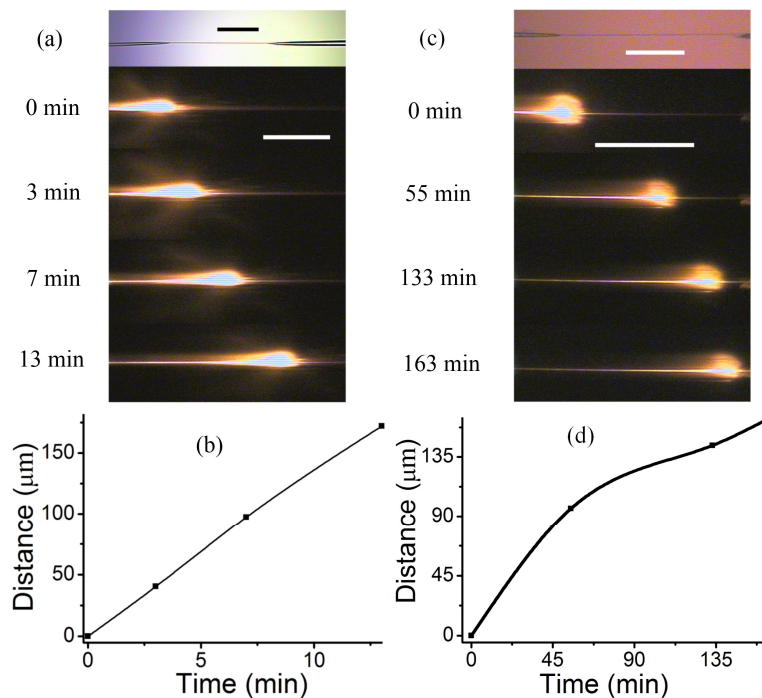

Fig. 2. PL images and graphs of PL moving distance vs. time of DNA-CTMA nanofiber and PMMA nanofiber. (a) Microscope images of a DNA-CTMA nanofiber (up first) and 4 captured images of the moving PL of the DNA-CTMA nanofiber (down others). (b) PL transmission distance vs. PL transmission time according to the PL transmission movie in (a). (c) Microscope images of a PMMA nanofiber (up) and 4 captured images of the moving PL of the PMMA nanofiber (down). (d) Graph of PL transmission distance and transmission time according to the PL transmission movie in (c). Scale bar: 200 μm (bright background), 100 μm (dark background).
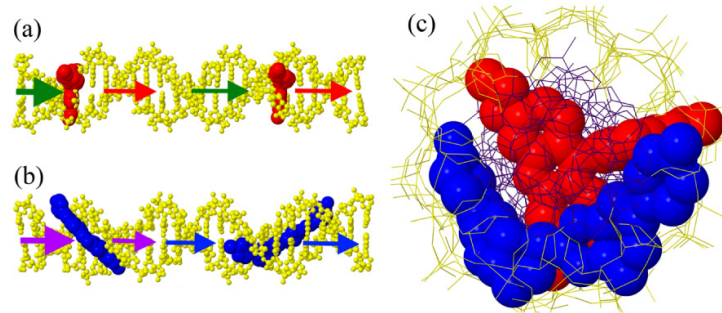
Fig. 3. 3D schematic illustration of DNA molecular waveguide. (a) 3D schematic model of DNA double strand with R6G (red molecules) intercalating. The green arrows show the transmission direction of excitation laser at wavelength of 532 nm and the red ones indicate the emitted PL. (b) 3D view of DNA double strand with Hoechst 33258 (blue molecules) binding. The laser (purple arrow) is at wavelength of 355 nm and the blue arrows indicate the emitted PL. (c) Sectional view comparison of anchor position difference of dye molecules in the DNA photonic wire. The DNA bases and the phosphate backbone are depicted by indigo rods and yellow rods, respectively. The phosphate backbone and bases are not illustrated with different colors in (a) and (b) so as to clearly show the dye molecules.
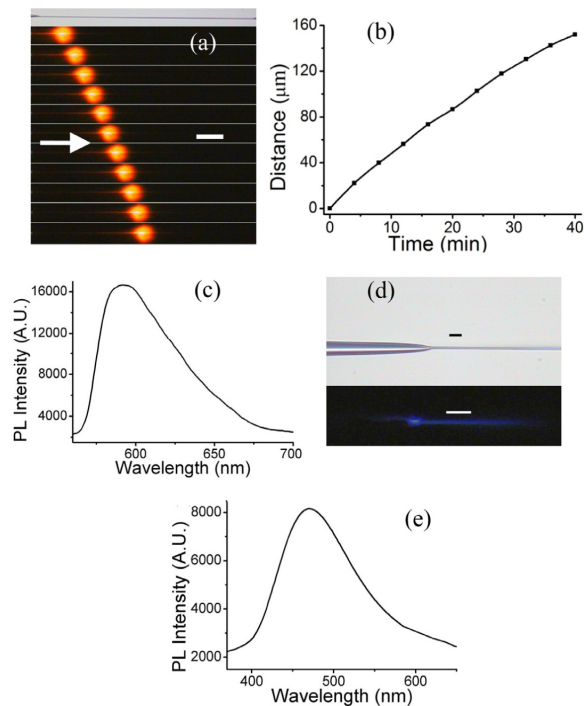

Fig. 4. PL images, graph of PL moving distance vs. time and spectra of dye-DNA molecular waveguide. (a) Microscopy images of the 1% R6G doped DNA nanofiber (about 600 nm in diameter) excited by 532 nm laser (63 µW) in dark background with 532 nm filter. Interval time of subplots: 4 minutes. Scale bar: 50 µm. (b) PL transmission distance vs. PL transmission time according to the PL transmission images in (a). (c) PL spectrum of the excited DNA nanofiber according to the PL transmission images in (a). (d) Microscopy image of a 1% Hoechst 33258 doped DNA nanofiber (about 540 nm in diameter) coupled with a taper in bright background (up, scale bar, 10 µm) and the image under 355 nm laser exciting (10 MHz pulsed laser, 70 nW) in dark background with 355 nm filter (down, scale bar, 10 µm). (e) PL spectrum of the DNA nanofiber in (d).

3. Tracing photon transmission in FRET-mediated DNA optical nanofibers

To further investigate the optical property of DNA-CTMA, we fabricated co-doped DNA-CTMA nanofibers from three dye mixed DNA solutions (the third dye is acriflavine). Acriflavine was also used as a small intercalator to study the steric hindrance in comparison with R6G. The steric hindrance was confirmed by that the concentration ratio of R6G to DNA-CTMA in the solution increased compared with its initial R6G concentration of about 1 wt % (half a milliliter) after hundreds of drawing. In contrast, such phenomenon did not occur for acriflavine. This may arise from the fact that R6G molecule is larger than acriflavine and relatively difficult to completely intercalate into the gap of base pairs. The two energy-level FRET includes energy transfer from Hoechst 33258-DNA-CTMA complexes to acriflavine-DNA-CTMA complexes as well as from acriflavine-DNA-CTMA complexes to R6G-DNA-CTMA. Figure 5a shows the PL microscope images.
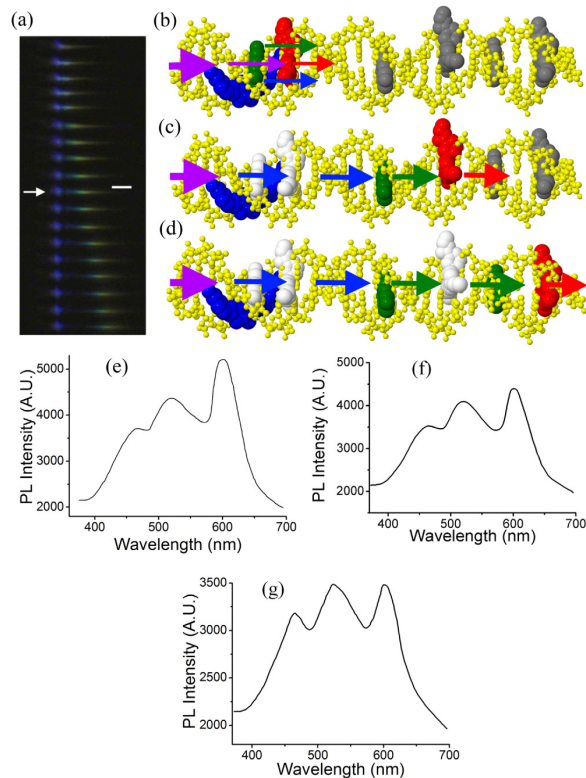

Fig. 5. FRET-mediated PL images in DNA molecular waveguide. (a) Microscopy images of three dyes doped DNA nanofiber (about 480 nm in diameter) excited by 355 nm laser (55 nW) in dark background with 355 nm filter. Interval time between two PL images: 10 minutes. Scale bar, 10 μm. (b) 3D schematic model of DNA (yellow atoms) with Hoechst 33258 (blue atoms), acriflavine (green atoms) and R6G (red atoms) attached. Purple arrows indicate 355 nm laser transmission. The blue, green and red arrows depict the PL emitted from Hoechst 33258, acriflavine and R6G, respectively. The gray are unreacted dye molecules. All colored arrows/symbols are the same below. (c) The same schematic model in (b) after being excited by 355 nm laser for certain time. White atoms: bleached dye molecules (the same below). (d) The same schematic model in (c) after three-color PL separation. (e) Normalized three-color PL spectrum except for the stationary coupling zone of the excited DNA nanofiber microscopy image on the top in (a) and also PL spectrum of (b). (f) Normalized three-color PL spectrum except for the PL in the stationary coupling zone of the excited DNA nanofiber microscopy image on the bottom in (a) and also PL spectrum of (c). (g) Normalized three-color PL spectrum except for the PL in the stationary coupling zone in (d).

We observed the FRET-assisted PL separating. The green and red PL surpassed the blue PL and the red run across the green gradually. The above phenomena did not result from the lifetime difference of two kinds of dyes as described as follows. When they were mixed, the molar ratio of Hoechst 33258, acriflavine and R6G was about 6 to 13 to 10 in solution, respectively. Referred to the fact that the lifetime of Hoechst 33258, acriflavine and R6G are about 3 ns, 4 ns and about 4 ns [36–38], Hoechst 33258 should decay more quickly than acriflavine and R6G. Based on the aforementioned analysis, we deduce FRET-assisted PL separation results from the following factors. As aforementioned, acriflavine and R6G anchored to the core of DNA molecular waveguide (see Fig. 3(c) and Figs. 5(b)-5(d)). At the beginning, they were co-excited by the excitation laser and the PL spectrum is shown in Fig. 5(e). Then R6G-DNA-CTMA complexes were bleached more quickly than Hoechst 33258-DNA-CTMA complexes and the change of the corresponding PL spectrum can be found in Fig. 5(f). In contrast, Hoechst 33258, as aforementioned, was excited with less energy density and so its bleaching rate was slow. Furthermore, in comparison with acriflavine, R6G has larger space and is relatively difficult to intercalate into DNA due to the influence of the steric hindrance as mentioned above. Accordingly, there were more half-intercalated R6G molecules with a short lifetime compared with acriflavine molecules even with a 2: 3 acriflavine-R6G ratio [39], which leads to its quicker bleaching rate and faster PL moving speed (Fig. 5(d)). As the PL was separating, the power of 355 nm laser to excite Hoechst 33258 increased and the direct excitation strength to R6G and acriflavine weakened gradually. As a result, the separated PL image keeps almost unchanged afterwards as can be seen in Fig. 5a. With the PL moving, the transmission loss increased and the intensity of the PL decreased, which is depicted in Figs. 5(e)-5(g). The separation of PL confirms the waveguide structure of DNA-CTMA molecule because such a phenomenon does not occur in similar scenario with other DNA photonic wire [5]. The stationary blue PL at the left end in Fig. 5(a), i.e. the coupling zone, results from the indirect excitation of Hoechst 33258 by the leaked excitation.

So far, many researches theoretically and experimentally indicate DNA-CTMA molecular waveguide has low transmission loss [9, 11]. Though the recent research found that there is mainly B form DNA in dye-doped biopolymer film in solution [39], the X-ray diffractometry reveals that the inter-helical distance of solid DNA-CTMA decreases significantly from theoretical 60 Å to 39.1 Å [40], which decreases the free energy in energy transfer so as to greatly enhance photon transmission and results in the lower transmission loss [41].

4. Conclusion

In summary, we probe photon transmission by comparing the interaction between the transmitting photons and the dyes anchoring to different positions of DNA-CTMA molecule. Based on the experimental results, we conclude that the DNA-CTMA is of molecular waveguide with inherently low loss and can be used as building blocks for molecular devices. This new finding will intrigue the applications of DNA molecular waveguide in optoelectronics area.

Acknowledgments